

Semi-supervised Optimal Transport with Self-paced Ensemble for Cross-hospital Sepsis Early Detection

Ruiqing Ding, Yu Zhou, Jie Xu, Yan Xie, Qiqiang Liang, He Ren,
Yixuan Wang, Yanlin Chen, Leye Wang and Man Huang

Abstract—The utilization of computer technology to solve problems in medical scenarios has attracted considerable attention in recent years, which still has great potential and space for exploration. Among them, machine learning has been widely used in the prediction, diagnosis and even treatment of Sepsis. However, state-of-the-art methods require large amounts of labeled medical data for supervised learning. In real-world applications, the lack of labeled data will cause enormous obstacles if one hospital wants to deploy a new Sepsis detection system. Different from the supervised learning setting, we need to use known information (e.g., from another hospital with rich labeled data) to help build a model with acceptable performance, i.e., transfer learning. In this paper, we propose a semi-supervised optimal transport with self-paced ensemble framework for Sepsis early detection, called *SPSSOT*, to transfer knowledge from the other that has rich labeled data. In *SPSSOT*, we first extract the same clinical indicators from the source domain (e.g., the hospital with rich labeled data) and the target domain (e.g., the hospital with little labeled data), then we combine the semi-supervised domain adaptation based on optimal transport theory with self-paced under-sampling to avoid a negative transfer possibly caused by covariate shift and class imbalance. On the whole, *SPSSOT* is an end-to-end transfer learning method for Sepsis early detection which can automatically select suitable samples from two domains respectively according to the number of iterations and align feature space of two domains. Extensive experiments on two open clinical datasets, MIMIC-III and Challenge (a challenge dataset from PhysioNet and CinC Challenge 2019), demonstrate that comparing with other methods, our proposed *SPSSOT*, can significantly improve the AUC values by at least 6% and 4% with only 1% labeled data in the target domain in two transfer learning scenarios, MIMIC→Challenge and Challenge→MIMIC.

Index Terms—Sepsis Early Detection, Optimal Transport, Data Imbalance, Semi-supervised Transfer Learning

1 INTRODUCTION

Sepsis is a life-threatening disease which occurs when body's response to infection is out of balance [1]. In severe cases, it will trigger body changes that may damage multiple organ systems and lead to death [2]. Sepsis has become a major cause of in-hospital death for intensive care unit (ICU) patients, which places an enormous burden on public health and health expenditures [3] [4]. According to statis-

tics, Sepsis is responsible for 10% of the ICU admissions and occupies about 25% of the ICU beds in US hospitals, accounting for over \$23.6 billion (6.2%) of total US hospital costs in 2013 [5]. Early diagnosis is crucial to proper sepsis management. Research shows that in a case of sepsis, each one hour delay in the administration of antibiotic treatment, the mortality rate increases by 7% [6].

Recently, more and more computer technology like machine learning has been widely applied in Sepsis's diagnosis and prediction. Some traditional classification algorithms, e.g., linear model [7], Support Vector Machine (SVM) [8], Neural Network [9], Gradient Boosting Decision Tree (GBDT) [10] and so on. All these are supervised machine learning methods, which need enough labeled data to achieve a good performance. In fact, it is common that one hospital has amounts of Electronic Medical Records (EMRs) of patients, while there are few EMRs have been labeled. Therefore, how to use these records to predict the health situations of new hospital patients is an important problem that still needs to be addressed. Transfer learning provides an unconventional perspective to transfer external knowledge from another hospital which has rich data with labels to improve the performance of current hospital [11]. It can also avoid expensive data-labeling costs at the same time. Some works tried transfer learning via fine-tuning parameters of pre-trained models [12] [13] [14]. However, we can not ignore the overfitting caused by fine-tuning a

- Ruiqing Ding and Leye Wang are with Key Lab of High Confidence Software Technologies (Peking University), Ministry of Education, China, and also with Department of Computer Science and Technology, Peking University, Beijing 100871, China.
E-mail: ruiqing@stu.pku.edu.cn, leye@pku.edu.cn
- Yu Zhou, Qiqiang Liang and Man Huang are with General Intensive Care Unit, Zhejiang University School of Medicine Second Affiliated Hospital, Hangzhou 310009, Zhejiang, China.
E-mail: {naseph, deter_leung, huangman}@zju.edu.cn
- Jie Xu is with IT center, Zhejiang University School of Medicine Second Affiliated Hospital, Hangzhou 310009, Zhejiang, China.
E-mail: 2202113@zju.edu.cn
- Yan Xie and He Ren are with Beijing HealSci Technology Co., Ltd., Beijing 100176, China.
E-mail: {yan.xie, he.ren}@healscitech.com
- Yixuan Wang is with Department of Computer Science and Technology, Peking University, Beijing 100871, China.
E-mail: kugamashiro@pku.edu.cn
- Yanlin Chen is with School of Information Management and Engineering, Shanghai University of Finance and Economics, Shanghai 200433, China.
E-mail: 1391469597@qq.com

(Equal Contribution: Ruiqing Ding and Yu Zhou, Corresponding author: Man Huang.)

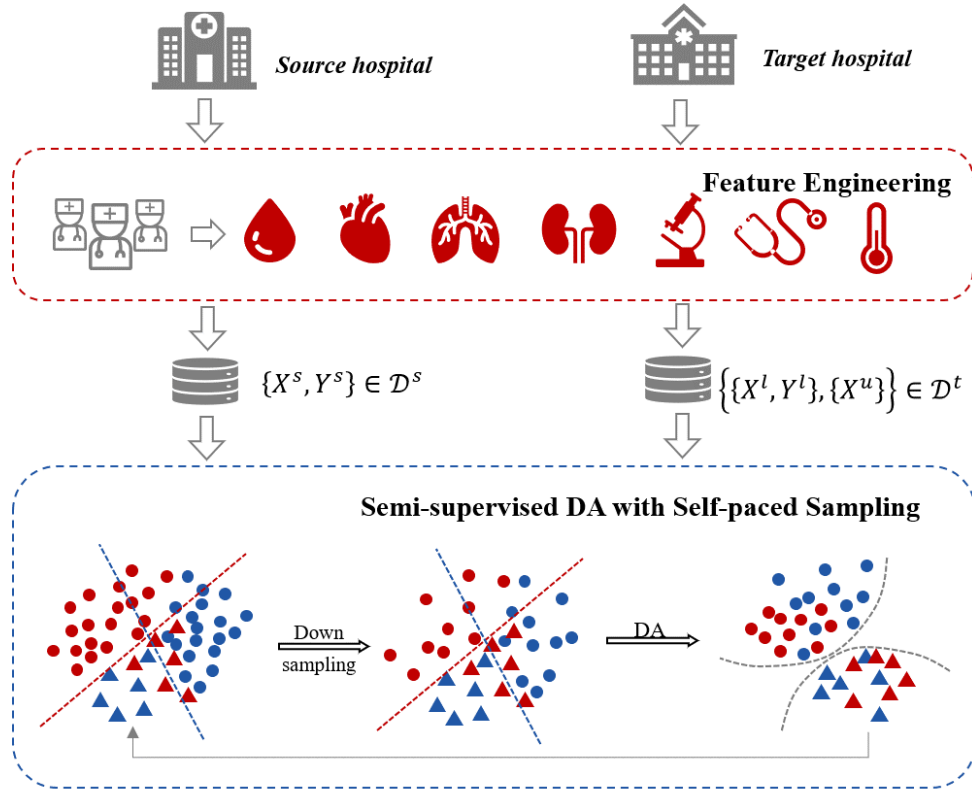


Fig. 1. The Overall Framework of Semi-supervised Optimal Transport with Self-paced Ensemble (SPSSOT), which includes 3 main parts: (1) Feature Engineering to extract Sepsis-related features under the guidance of doctors; (2) Self-paced sampling. The proportion of data with no sepsis in the original data is significantly higher than that with sepsis. To solve the negative effects of extreme data imbalance, we using this method to filter out “more contributing” samples from negative samples (no Sepsis, shown as circles), which will help to improve the performance of classifier; (3) DA (Semi-supervised domain adaptation): given all data with labels of source hospital (shown as red), little data with labels and most data without labels in target hospital (shown as blue), using optimal transport to align two feature spaces and learn a better classifier to distinguish whether Sepsis occurs. *Best viewed in color.*

large number of parameters with very small labeled data [15].

Consequently, it is still challenging to achieve successful knowledge transfer, especially in clinical data, due to the following reasons:

Covariate Shift. First, different hospitals may have different medical instruments which will lead to different test values. Also, patients’ agglomeration is another factor that cannot be neglected. The choice of hospital is influenced by the hospital quality measured in terms of patient outcomes [16], which means patients tend to choose a hospital that is more suitable for their diseases and health conditions. These will make patients’ information from two hospitals are significantly different; in other words, they are not in the same feature space. Hence it is necessary to map them into a common hidden space, which is also described as domain adaptation [17].

Label shift. Label-shift scenarios appear in variously practical machine learning problems which means the label distribution changes from source to target [18]. In particular, the incidence of a disease may change over locations and time, which is very easy to result in a negative transfer as well. Some methods have been proposed to estimate the importance weights of the source samples [19] [20],

however, they result in a massive computational burden for large sample size problems. Therefore, it is still worth exploring that how to use the obtained knowledge from a different hospital with data abundance to detect the disease in the new target hospital in an efficient way.

Class Imbalance. Imbalanced data is ubiquitous in the real world, which exhibits long-tailed distributions [21], especially in medical diagnosis datasets, whose unbalanced ratios can reach 1:10 or even higher [22]. While realizing the domain adaptation task, how to reduce the classification bias caused by data imbalance and find a more suitable decision boundary is also an important issue that needs to be solved.

To overcome the above difficulties, we proposed a semi-supervised optimal transport with self-paced ensemble method to solve cross-hospital Sepsis early detection. There are **three main components** of this method: *feature engineering* under the guidance of doctors to extract features correlated with Sepsis, *self-paced ensemble* to downsampling from majority data automatically to achieve data balance, and *semi-supervised domain adaptation with optimal transport* to solve the problem of different feature distribution. The overall framework is shown in Fig. 1. The contributions of this paper are summarized as follows:

(1) To the best of our knowledge, this is the first work on cross-hospital Sepsis early detection. In particular, by properly transferring knowledge from another hospital that has rich data with Sepsis labels, our method can achieve relatively good detection performance even if the target hospital has little labeled data.

(2) Considering the different feature distributions, the extremely unbalanced and noisy data status in the cross-hospital Sepsis early detection problem, we propose a novel end-to-end deep transfer learning framework, called *SPSSOT*, with three components, feature engineering, semi-supervised domain adaptation with optimal transport, and self-paced ensemble. More specifically, in *semi-supervised domain adaptation with optimal transport*, we devise a label adaptive optimal transport strategy to achieve the precise-pairwise optimal transport and an intra-domain discriminative centroid utilization strategy to learn deep discriminative features for a better decision boundary. In *self-paced ensemble*, to tackle the problem of class imbalance, we improve and merge an ensemble algorithm for imbalanced classification [23] into our deep transfer learning method to automatically downsample from both domains' majority data.

(3) By conducting the experiments on the two transfer directions between two open clinical datasets, MIMIC and Challenge, we have verified that our proposed *SPSSOT*, with only 1% labeled data in the target domain, can increase the AUC values by at least 6% and 4%, compared to state-of-the-art transfer learning methods [24]. Also, as the number of labeled samples in the target domain decreases, our method works stably and outperforms existing methods.

2 RELATED WORK

This paper mainly provided a new solution for Sepsis early detection when there are few labeled EMRs in the hospital. We proposed a transfer learning framework based on optimal transport theory [25] [26] to solve data discrepancy between different hospitals. At the same time, we introduced a self-paced ensemble method to address the extremely label imbalance problem which is common in medical data. Therefore, we provide a brief overview of related work in three fields, Sepsis early detection, transfer learning with optimal transport and data imbalance.

2.1 Sepsis Early Detection

Machine learning (ML) techniques excel in the analysis of complex signals in data-rich environments which promise to improve the early detection of Sepsis. Most of the studies are carried out in the ICU [27] [28]. Systematic review and meta-analysis show that individual machine learning models can accurately predict Sepsis onset ahead of time on retrospective data. The PhysioNet/Computing in Cardiology (CinC) Challenge 2019 addresses this issue and promotes the development of open-source AI algorithms for real-time and early detection of Sepsis [29]. Some work adopts Gradient Boosting Decision Tree (GBDT) to achieve superior performance for predicting Sepsis risk in a real-time way and Shapley Additive exPlanations (SHAP) to provide the interpretable information for understanding Sepsis risk in ICU [10] [30]. There is also research that summarizes

the reinforcement learning model which provided individualized and clinically interpretable treatment decisions for Sepsis that could improve patient outcomes [31]. Such approaches typically apply machine learning techniques to clinical data that can dynamically suggest real-time predictions and optimal treatments for adult patients with sepsis and yield unusually brilliant results in the medical field. In addition, machine learning models have also been used in ICU to predict pathologies such as acute kidney injury [32], circulatory failure [33], Bleeding Independently associated with Mortality [34], and hypotensive events [35]. However, there are still few kinds of research working on Sepsis early detection without enough labeled data.

2.2 Transfer Learning with Optimal Transport

The core of transfer learning is to align the source and target distributions by minimizing a divergence that measures the discrepancy between them. Optimal Transport (OT) theory can be regarded as one of the discrepancy-based alignment methods because it can be used for computing Wasserstein distances (also called Monge-Kantorovich or Earth Mover distances) between probability distributions [36]. Given the cost function (like l_2 distance) between samples from source and target domains, we can compute the probabilistic coupling matrix γ . It has been applied in domain adaptation to learn the transformation between different domains [37] [38], with associated theoretical guarantees [39]. Also, it is suitable for different transfer scenarios, i.e. unsupervised [40] and semi-supervised [41] situations. Initially, limited by the space complexity of OT (super-quadratically with the size of the sample), it can only be used to solve problems of small or medium size [42]. In recent years, more and more work has tried to combine deep learning method and optimal transport, and train through multiple rounds of minibatch iterative optimization, like Deep Joint Optimal Transport (DeepJDOT) [24] and Reliable Weighted Optimal Transport (RWOT) [43], which break the limit of complexity. While realizing domain alignment, these training processes make sure that good semantic representation can be learned for downstream tasks such as classification.

In our setting, few labeled patients are available in the target hospital, which can be seen as a problem of semi-supervised transfer learning. Unlike common methods for the unsupervised situation, we can further consider the coupling constraints for labeled samples when using OT.

2.3 Data Imbalance

Learning from imbalanced data is a topic with a long history. Traditionally, machine learning algorithms (e.g., SVM [44], Neural Networks [45]) may assume that the number of samples in considered classes are roughly the same, which is not the case in many real-life problems, medical issues for example. In many medical datasets, the ratio of minority class to majority class can be 1:10, even up to 1:50 [22]. The key point of imbalanced learning is that the minority classes are often more important with more essential information, under the background of medical datasets, that is to say, we need to focus on the diseased samples rather than the healthy samples.

Over the last two decades, a series of studies have been proposed to overcome imbalanced data learning issues, which can mainly be classified into three different approaches: data-level methods, algorithm-level methods, and the combination of the two.

Data-level methods modify the dataset to balance the minority and the majority. A typical way is to remove some samples from the majority class (undersampling) or produce some samples that are similar to the minority samples (oversampling). Algorithm-level methods do not change the dataset directly; rather, they modify the algorithm to enhance the attention of the model to the minority class, for example, setting cost matrix in cost-sensitive learning with some assistance of domain experts before-hand [46]. [47] proposed a new loss function Focal Loss address the one-stage object detection scenario in which there is an extreme imbalance foreground and background classes during training, significantly approved the accuracy of one-stage detectors.

Many methods take the advantage of the previous two, combine one of the data-level or algorithm-level methods with some state-of-art machine learning method. SMOTE-Boost [48] combined SMOTE [49] with Boosting [50] ensemble learning to gain a strong ensemble classifier. SPE [23] tried to handle tasks on the highly imbalanced, noisy and large-scale dataset by introducing the “classification hardness” function (any function that can calculate the loss/error of a single sample) and using under-sampling with an iterated strategy to perform boosting-like serial training to obtain an additive model.

3 PRELIMINARIES

In this section, we first formulate our research problem from the application perspective. Then, we abstract our problem in the transfer settings.

3.1 Sepsis Early Detection

The objective of this work is to use patients’ demographic and physiological data for Sepsis early detection. Considering the early warning of Sepsis is potentially life-saving, we will predict sepsis 6 hours before the clinical prediction of Sepsis, as the setting of the PhysioNet Computing in Cardiology Challenge 2019 [29] [51] whose topic is *Early Prediction of Sepsis from Clinical Data*¹. The PhysioNet Computing in Cardiology Challenges are the most important challenges in the global physiological measurement, clinical data analysis, and cardiovascular disease detection applications, which have attracted many teams to participate in every year.

In short, given a set of n patients’ clinical variables since they entered the ICUs $\{\mathcal{X}_1, \mathcal{X}_2, \dots, \mathcal{X}_n\}$, where the i -th patient’s is $\mathcal{X}_i = \langle \mathbf{x}_1, \mathbf{x}_2, \dots, \mathbf{x}_m \rangle$, where \mathbf{x}_j is the clinical features of j -th time windows (we set the length of time window as 6 hours). Then we can predict whether Sepsis will occur in the next 6 hours for each \mathbf{x}_j . Therefore, it can be seen as a binary classification problem. The clinical variables will be explained in detail in Sec. 4.1.

3.2 Semi-supervised Transfer Learning Formulation

When we try to build the detection model in a hospital that has enough historical data however with few Sepsis labels, the intuitive solution is to learn knowledge from other rich data sources and utilize it in the current hospital. In other words, we can regard this problem as the scenario of semi-supervised transfer learning.

In details, we are given a source domain and a target domain, which have the same features. The source domain contains a large number of labeled samples, and the target domain only contains a limited number of labeled samples (i.e. the most samples are unlabeled). The task is to improve the classification performance in the target domain. To simplify representation, we denote source domain as $\mathcal{D}^s = \{(\mathbf{x}_i^s, y_i^s) | i = 1, 2, \dots, n_s\}$, $\mathbf{x}_i^s \in \mathbb{R}^{d_s}$. And target domain is $\mathcal{D}^t = \{\mathcal{D}^l, \mathcal{D}^u\}$, where $\mathcal{D}^l = \{(\mathbf{x}_j^l, y_j^l) | j = 1, 2, \dots, n_l\}$ and $\mathcal{D}^u = \{(\mathbf{x}_k^u) | k = 1, 2, \dots, n_u\}$, $\mathbf{x}_j^l \in \mathbb{R}^{d_t}$, $(\mathbf{x}_k^u) \in \mathbb{R}^{d_t}$. n_l and n_u are the number of labeled and unlabeled target samples, respectively, $n_t = n_l + n_u$ ($n_l \ll n_u$). Also, we have $d_s = d_t$ and $\mathcal{Y}^s = \mathcal{Y}^t = \{0, 1\}$

4 METHODOLOGY

In this section, we propose a semi-supervised transfer learning framework to address our research problem, whose schematic diagram is illustrated as Fig.1. It consists of 3 main parts: (1) Feature Engineering; (2) Semi-supervised Optimal Transport; (3) Self-paced ensemble. We will elaborate on each part below.

4.1 Feature Engineering

We use the same clinical variables and sepsis criteria which are extracted from the Electronic Medical Records (EMRs). For each patient, there are 35 clinical variables, including 7 vital sign variables(HR, O2Sat, Temp, SBP, MAP, DBP, Resp), 24 laboratory variables(BaseExcess, HCO3, FiO2, pH, PaCO2, SaO2, AST, BUN, Alkalinephos, Calcium, Chloride, Creatinine, Glucose, Lactate, Magnesium, Phosphate, Potassium, Bilirubin_total, direct bilirubin, Hct, Hgb, PTT, WBC, Platelets), and 4 demographic variables(Sex, Age, HospAdmTime, ICULOS). These variables are selected measurements in a 6-hour sliding window. The Sepsis-3 criteria for sepsis are extracted as suspected infection with associated organ dysfunction (SOFA ≥ 2) [52] [1]. The clinical criteria are used to confirm sepsis onsets per 6-hour. For each vital sign and laboratory value in each patient record, most vital signs are updated on an hourly basis in most patient records, and most laboratory values are updated on a daily basis.

The sepsis incidence rate varies with respect to the ICU-LOS(i.e., time stay in ICU). At the early phase, the incidence rate is moderate and slightly increases probably due to the patient prior conditions; at the middle phase, the incidence rate drops a little and becomes stable at a level lower than that of the early phase and the incidence rate increases drastically at late phase because of the smaller number of the total number of instances and the bigger vulnerability of the patients for staying long in ICU [10]. Typical vital signs including heart rate (HR), oxygen saturation (O2Sat), body temperature (Temp), mean arterial blood pressure (MAP),

1. <https://physionet.org/content/challenge-2019/1.0.0/>

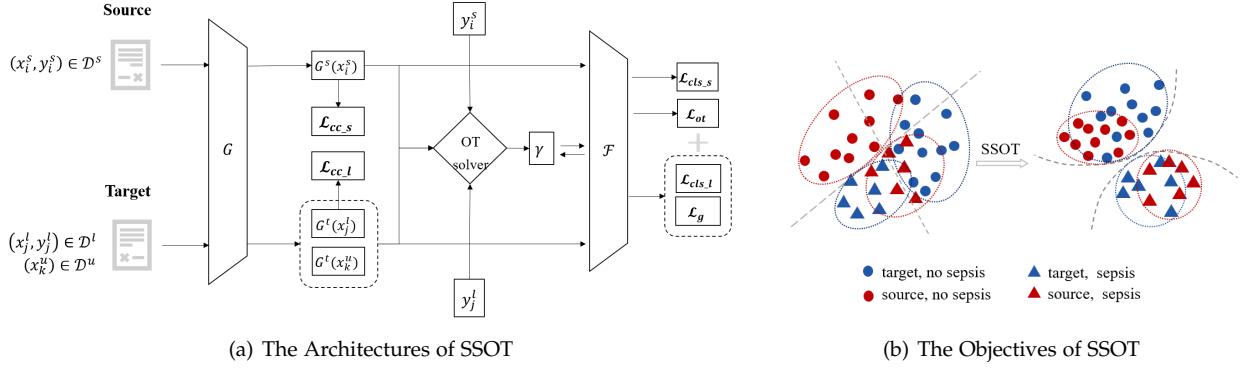


Fig. 2. Semi-supervised Domain Adaptation with Optimal Transport (SSOT).

Algorithm 1 Semi-supervised Optimal Transport (SSOT)

Require: Source data as $\mathcal{D}^s = \{(x_i^s, y_i^s)\}_{i=1}^{n_s}$; Target labeled data as $\mathcal{D}^l = \{(x_j^l, y_j^l)\}_{j=1}^{n_l}$; Target unlabeled data as $\mathcal{D}^u = \{(x_k^u)\}_{k=1}^{n_u}$; T is set as the total number of training iterations; n represents the batch-size for training.

- 1: Initialize the feature generator \mathcal{G} and the classifier \mathcal{F} by fine tuning;
 - 2: **for** $i = 1$ to T **do**
 - 3: Randomly select half of source samples and target labeled samples;
 - 4: Calculate the class centers in two domains according to Eq.8.
 - 5: Randomly choose source samples $\{(x_i^s, y_i^s)\}_{i=1}^{n_s}$, target labeled samples $\{(x_j^l, y_j^l)\}_{j=1}^{n_l/2} \in \mathcal{D}^l$, and target unlabeled samples $\{(x_k^u)\}_{k=1}^{n_u/2} \in \mathcal{D}^u$;
 - 6: Fix $\hat{\mathcal{G}}$ and $\hat{\mathcal{F}}$, solve for γ ;
 - 7: Fix $\hat{\gamma}$, update parameters of \mathcal{G} and \mathcal{F} ;
 - 8: **end for**
 - 9: **return** \mathcal{G} and \mathcal{F} ;
-

and respiratory rate (Resp) impact on prediction are shown over time [30] [29].

4.2 Semi-supervised Optimal Transport

Optimal transport theory has been used in many transfer learning researches, especially unsupervised transfer learning [36]. However, few labeled samples in the target domain are more in line with the actual situation, specifically the medical diagnosis problem. We tend to label some data to achieve better performance, though we may pay a small cost.

Based on this motivation, we proposed semi-supervised optimal transport (SSOT) to implement domain adaptation, whose goal is to design a neural network that enables end-to-end training of a transferable feature generator and an adaptive classifier to achieve better classification performance as well as minimize the distribution discrepancy across domains, as illustrated in Fig. 2. Because the clinical features can be seen as tabular data, we choose classical multi-layer perception (MLP) with shared weights as the feature generator \mathcal{G} .

The main parts of SSOT are label adaptive optimal transport, group entropic loss for unlabeled samples and intra-domain discriminative centroid utilization. In the following sections, we present the details of SSOT.

4.2.1 Label Adaptive Optimal Transport

We have few labeled samples in the target domain means that there is more information that can be exploited than

unsupervised domain adaptation methods. Therefore, we can design a mechanism that makes sure *samples in the target domain should only be matched with samples in the source domain that have the same labels*.

Optimal Transport. The optimization of optimal transport is based on Kantorovich problem [53] which seeks for a general coupling $\gamma \in \mathcal{X}(\mathcal{D}^s, \mathcal{D}^t)$ between \mathcal{D}^s and \mathcal{D}^t :

$$\gamma^* = \arg \min_{\gamma \in \mathcal{X}(\mathcal{D}^s, \mathcal{D}^t)} \int_{\mathcal{D}^s \times \mathcal{D}^t} \mathcal{C}(x^s, x^t) d\gamma(x^s, x^t) \quad (1)$$

where $\mathcal{X}(\mathcal{D}^s, \mathcal{D}^t)$ denotes the probability distribution between \mathcal{D}^s and \mathcal{D}^t .

The discrete reformulation is

$$\gamma^* = \arg \min_{\gamma \in \mathcal{X}(\mathcal{D}^s, \mathcal{D}^t)} \langle \gamma, \mathcal{C} \rangle_F \quad (2)$$

where $\langle \cdot, \cdot \rangle_F$ is the Frobenius dot product, $\mathcal{C} \in \mathbb{R}^{n_1 \times n_2}$ is the cost function matrix. And $\mathcal{C}(x^s, x^t) = \|x^s - x^t\|^k$ ($k = 2$) represents the cost to move probability mass from x^s to x^t .

Label Adaptive Constraint. We adjust the cost of transport according to the labels of the two domains' samples. If two samples with the same labels, we can ignore the transport cost between them, i.e., $\mathcal{C}(x^s, x^t) = 0$, if $y^s = y^t$. At the same time, for unlabeled target samples, we can consider supplementing a weight for transport cost to measure the difference between the predicted probabilities and the labels of source samples. To achieve this goal, we design a reweight matrix, also can be called the label adaptive matrix,

\mathcal{R} . Therefore, the label adaptive optimal transport can be written as

$$\gamma^* = \arg \min_{\gamma \in \mathcal{X}(\mathcal{D}^s, \mathcal{D}^t)} \langle \gamma, \mathcal{R} \cdot \mathcal{C} \rangle_F \quad (3)$$

where $\mathcal{R}(x^t, x^s) = \begin{cases} |y(x^s) - y(x^t)| \in \{0, 1\}, & (x^t, y^t) \in \mathcal{D}^t; \\ |y(x^s) - \hat{y}(x^t)| \in [0, 1], & x^t \in \mathcal{D}^u \end{cases}$

Therefore, the solution to this problem can be described to minimize the following objective function

$$\mathcal{L}_{lot} = \sum_{i,j} \alpha \gamma_{i,j}^* (\|G(x_i^s) - G(x_j^t)\|^2) + \mathcal{L}_{cls} \quad (4)$$

where \mathcal{L}_{cls} is cross entropy function, i.e.

$$\begin{aligned} \mathcal{L}_{cls} &= \theta_s \mathcal{L}_{cls}^s + \mathcal{L}_{cls}^l \\ &= -\theta_s \sum_{x_i^s \in X_s} y'(x_i^s) \log y(x_i^s) \\ &\quad - \sum_{x_j^l \in X_l} y'(x_j^l) \log y(x_j^l) \end{aligned} \quad (5)$$

4.2.2 Group Entropic Loss for Unlabeled Samples

Because target unlabeled samples have no labels, it is difficult to judge whether the predicted results are accurate or not. Here, we try to borrow the labels of the source domain to calculate the classification loss of unlabeled samples. If one target sample x_j^u has a high transport probability from one source sample x_i^s , in other words, γ_{ij} is high, then we would like that the predicted label is the same with $y_{x_i^s}$ as much as possible.

Therefore, we can calculate the group entropic loss to portray this relationship, whose form is to compare the cross entropy between the predicted probability of each target unlabeled sample and the true label of each source sample. It can be written as

$$\mathcal{L}_g = -\frac{1}{n_s} \frac{1}{n_u} \sum_{x_i^s \in X^s} \sum_{x_j^u \in X^u} \gamma_{ij}^* (y_{x_i^s} \log \hat{y}_{x_j^u}) \quad (6)$$

where $\hat{y}_{x_j^u} = \mathcal{F}(\mathcal{G}(x_j^u))$ is the predicted probability of x_j^u . By penalizing couplings with high cross entropies, we can achieve that each unlabeled target sample can be transported from source samples that have the same class.

4.2.3 Intra-domain discriminative centroid utilization

Intra-domain discriminative centroid utilization is to make sure that samples belonging to the same class can be as closer as possible in the feature space, which can help to find a better classification boundary. Inspired of the center loss [54], we consider the discriminative centroid loss \mathcal{L}_{cc} for the samples with labels in both source domain and target domain.

$$\begin{aligned} \mathcal{L}_{cc} &= \frac{1}{n_s} \sum_{i=1}^{n_s} \|\mathcal{G}(x_i^s) - c_{y_i^s}^s\|_2^2 - (\|c_0^s - c_1^s\|_2^2) \\ &\quad + \frac{1}{n_l} \sum_{j=1}^{n_l} \|\mathcal{G}(x_j^t) - c_{y_j^t}^t\|_2^2 - (\|c_0^t - c_1^t\|_2^2) \end{aligned} \quad (7)$$

where $c_{y_i^s}^s$ and $c_{y_j^t}^t$ denote the y_i^s -th and y_j^t -th class center in the source domain and target domain, respectively. We

evaluate them by averaging deep features of some samples as

$$\begin{aligned} c_k^s &= \frac{1}{S_a} \sum_{i=1}^{N_a} \mathcal{G}(x_i^s) \mathcal{I}(y_i^s, k) \\ c_k^t &= \frac{1}{S_b} \sum_{j=1}^{N_b} \mathcal{G}(x_j^t) \mathcal{I}(y_j^t, k) \end{aligned} \quad (8)$$

where $\mathcal{I}(y_i, k) = \begin{cases} 1, & y_i = k; \\ 0, & o.w. \end{cases}$, $k \in \{0, 1\}$ and $S_a = \sum_{i=1}^{N_a} \mathcal{I}(y_i^s, k)$, $S_b = \sum_{j=1}^{N_b} \mathcal{I}(y_j^t, k)$. Ideally, the class centers should be calculated based on all the samples while the procedure is time-consuming. Herein, we compute the class centers using N_a and N_b samples. In experiments, we set $N_a = 0.5 \times n_s$, $N_b = 0.5 \times n_l$.

4.2.4 Training

Here, we introduce the training process of SSOT. Considering the three parts of SSOT, the training objective can be described as

$$\min_{\mathcal{G}, \mathcal{F}} \mathcal{L}_{lot} + \lambda \mathcal{L}_g + \beta \mathcal{L}_{cc} \quad (9)$$

where λ and β denote hyper-parameters that respectively trade-off the contribution of the intra-domain structures and domain alignment.

The training process is shown in Algorithm 1. Especially, in each iteration, we use two steps to update the parameters: firstly, we should fix the feature generator \mathcal{G} and the classifier \mathcal{F} and using a toolbox, POT (python optimal transport) [42], to calculate the coupling γ (line 6); Then we fix γ to update \mathcal{G} and \mathcal{F} with stochastic gradient (line 7).

4.3 Self-paced Ensemble

When we try to transfer knowledge from the source domain to the target domain, it is very common to occur label shift between two domains [36]. At the same time, it is ubiquitous that medical diagnostic data is extremely imbalanced which reveals not only the disproportion between classes but also other difficulties embedded in the nature of data, such as, *noises and class overlapping* [55].

Therefore, it is necessary to design a sampling strategy to solve both problems. Inspired by self-paced ensemble method (SPE) [23], We improve this algorithm to adapt it to a deep end-to-end prediction framework and we can achieve to sample simultaneously from labeled samples of two domains in our scenario. Fig.3 shows the basic idea of self-paced ensemble. Next, we will introduce in detail how the sampling strategy is implemented.

4.3.1 Classification Hardness Function

We use \mathcal{H} to denote the hardness function, which can be calculated by the summation of individual sample errors, such as absolute error, squared error, cross entropy, etc. Given a classifier \mathcal{F} and a sample (x, y) , the hardness can be written as $\mathcal{H}(x, y, \mathcal{F}) = |\mathcal{F}(x) - y| \in [0, 1]$. This value contains information that is highly associated with the difficulty of the classification, like noise and model capacity.

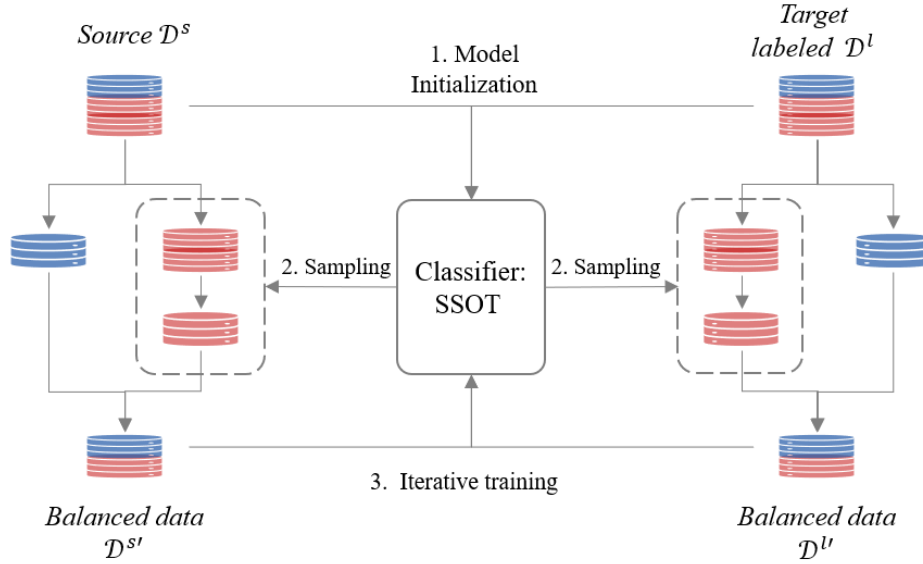


Fig. 3. The Basic Idea of Self-paced Ensemble Based on SSOT (SPSSOT). There are 3 main steps: (1) Initialize SSOT according to Algorithm 1; (2) Self-paced under-sampling from majority class in both domains to obtain balanced data; (3) Get an additive model by iteration training. *Best viewed in color.*

Algorithm 2 Semi-supervised Optimal Transport with Self-paced Ensemble (SPSSOT)

Require: Source data as $\mathcal{D}^s = \{(\mathbf{x}_i^s, y_i^s)\}_{i=1}^{n_s}$; Target labeled data as $\mathcal{D}^l = \{(\mathbf{x}_j^l, y_j^l)\}_{j=1}^{n_l}$; Target unlabeled data as $\mathcal{D}^u = \{(\mathbf{x}_k^u)\}_{k=1}^{n_u}$; Hardness function \mathcal{H} ; Base classifier SSOT; Number of base classifiers n ; Number of bins k ; Total number of training iterations of SSOT T ;

- 1: Initialize $SSOT_0$ according to Algorithm 1;
 - 2: **for** $i = 1$ to n **do**
 - 3: Ensemble $F_i(\mathcal{D}^s, \mathcal{D}^l, \mathcal{D}^u) = \frac{1}{i} \sum_{j=0}^{i-1} SSOT_j(\mathcal{D}^s, \mathcal{D}^l, \mathcal{D}^u)$;
 - 4: **for** $\mathcal{D} \in \{\mathcal{D}^s, \mathcal{D}^l\}$ **do**
 - 5: Initialize $\mathcal{P} \leftarrow$ minority in \mathcal{D} ;
 - 6: Cut majority set into k bins w.r.t. $\mathcal{H}(\mathcal{D}, F_i)$: B_1, B_2, \dots, B_k ;
 - 7: Average hardness contribution in l -th bin: $h_l = \sum_{m \in B_l} \mathcal{H}(x_m, y_m, F_i) / |B_l|, \forall l = 1, \dots, k$;
 - 8: Update self-paced factor $\omega = \tan(\frac{i\pi}{2n})$;
 - 9: Unnormalized sampling weight of l -th bin: $p_l = \frac{1}{h_l + \omega}, \forall l = 1, \dots, k$;
 - 10: Under-sample from l -th bin with $\frac{p_l}{\sum_m p_m} \cdot |\mathcal{P}|$;
 - 11: **end for**
 - 12: Train $SSOT_i$ using newly under-sampled subset according to Algorithm 1;
 - 13: **end for**
 - 14: **return** final ensemble $F(\mathcal{D}^s, \mathcal{D}^l, \mathcal{D}^u) = \frac{1}{n} \sum_{m=1}^n SSOT_m(\mathcal{D}^s, \mathcal{D}^l, \mathcal{D}^u)$;
-

According to the hardness values, we can divide samples into three types as follows:

- *Trivial samples* account for the largest proportion and are easy to classify, i.e., each of them only contributes tiny hardness. However, the overall contribution can not be ignored due to its large population.
- *Noise samples* are different from trivial samples. Though the population is small, each of them has a large hardness value. These samples can be caused by the distinguishable overlapping and will exist stably even when the model is converged.
- *Borderline samples* are the rest that provide lots of information while training a classification model.

Intuitively, while sampling, we should (1) keep a small proportion of trivial samples to maintain the original dis-

tribution to avoid overfitting; (2) exclude the interference of noise samples as much as possible during training; (3) enlarge the weights of borderline samples to improve the model performance. The problem still needs to address is how to distinguish the samples and achieve under-sampling in practice.

4.3.2 Self-paced Under-sampling

There are two important components, *self-paced hardness harmonize* and *combination with SSOT* while achieving self-paced sampling and iterative training. Algorithm 2 gives the detailed process.

Self-paced hardness harmonize. We regard the class with a high proportion as the *majority*. After calculating the hardness values of the majority samples, we can split them into k bins which indicate different hardness levels.

Then we can under-sample from every bin by ensuring the total hardness contribution of each bin is the same, as well as to generate a balanced dataset [23]. By harmonizing hardness contribution, the sample probability in those bins with a large population will decrease. However, the samples we focus on will change with the number of iterations. In the beginning, we tend to pay more attention to borderline samples to improve the generalization of our model. While in the later iterations, the trivial samples will be more important than before to avoid overfitting. Therefore, we keep the self-paced factor ω to further adjust the weight of each bin. Here, we use *tan* function to control the change of ω (line 8 of Algorithm 2).

Combination With SSOT. Unlike the setting of SPE [23] which adapts the most classification models of sklearn ², we should solve the data imbalance in two domains and combine the self-paced ensemble strategy with SSOT based on deep learning. As shown in Fig.3, we replace the basic models with SSOT as the base classifier and perform self-paced under-sampling in parallel on source data and target labeled data to obtain two balanced datasets for the next iteration.

5 EXPERIMENTS

5.1 Dataset

There are two datasets we use in the experiments, **MIMIC-III** [56] and the dataset from the PhysioNet Computing in Cardiology Challenge 2019 [29], called **Challenge** in this paper. To achieve our prediction, we extracted the datasets within 48 hours since patients entered ICUs. Because a part of patients' records have too many missing values, we screened out patients whose missing value ratio is less than 80%. To obtain the dynamic change information of the data over a period of time, for every patient, we calculated the maximum, minimum, mean, standard error and latest of each clinical indicator within 6 hours, like heart rate and blood pressure. Then we can aggregate these statistical values as a sample (or a record). Through such preprocessing, we obtain the final data for experiments. Some basic statistic information has been enumerated in Table 1.

TABLE 1
Statistics of the Datasets Used in the Experiment

	MIMIC	Challenge
# patients	12529	8270
# septic patients	2977	1831
Sepsis prevalence (%)	23.76	22.14
# samples	87501	45674
# samples occur Sepsis in next 6 hours	5032	4869
samples with sepsis (%)	5.75	10.66

5.2 Compared Algorithms

In experiments, we split target data into three parts: 1% as labeled data (we will change the label ratio later in Sec.

5.5.3), 79% as unlabeled data, and the left 20% as test data. To demonstrate the effectiveness of our method, we include four types of baselines for comparison in our experiments.

- *Source only*: only use all the source data to train a classifier and directly evaluate it with the target test data.
- *Target only*: only use little labeled data (i.e., 1%) in the target domain to train a classifier and evaluate it with the target test data.
- *Source & Target Train Together*: put the source data and the labeled target data together as training data to learn a classifier.
- *Source & Target Transfer*: instead of training together, design specific transfer learning methods to transfer knowledge from the source domain to the target domain.

In the former three types, we all use three classical machine learning algorithms which have been widely used in sepsis early detection.

- *LR* [7]: Logistic Regression, a basic and widely-used classification method.
- *NN* [9]: Neural Network, a deep learning method which has attracted more and more attention in recent years.
- *XGBoost* [57]: a model widely used in medical diagnosis problems.

While we try to transfer knowledge from the source domain, there are three methods for comparison.

- *DeepJDOT* [24]: an unsupervised domain adaptation method that does not need any labeled target data.
- *Finetune*: fine-tuned NN, which is first trained on the source data, and then fine-tune with the target labeled data.
- *SPSSOT*: it is our method proposed in Sec. 4 which is a semi-supervised domain adaptation method.

5.3 Experiment Design

There is a self-paced sampling strategy in *SPSSOT* to solve the class imbalance question. For a fair comparison, we also apply the method, *SPE* ³, to achieve down-sampling of majority data and train ensemble models when using *LR*, *NN* and *XGBoost* as base classifiers, where the hardness function is set to Squared Error, the number of base classifiers is set to 20 and the number of bins is to 15. *LR* and *XGBoost* are trained with default parameters, and *NN* has three hidden linear layers, whose dimension is (256, 128, 128).

In transfer methods, we use two linear layers as the feature generator \mathcal{G} and the dimension is (256, 128). The structure of classifier, \mathcal{F} , is also two-layer and the dimension is (128, 2), where 2 means that there are two classes in our task. The batch size is set to 128, the parameter optimization algorithm is SGD, and the learning rate is set to 0.001. In *Finetune*, we first train \mathcal{G} and \mathcal{F} with source data and fine-tune them with target labeled data, both parts will train 100 epoches. In *DeepJDOT* ⁴, we set $\alpha = 0.5$, $\lambda_t = 1.0$, $\lambda_s = 2.0$

3. <https://github.com/ZhiningLiu1998/self-paced-ensemble>

4. <https://github.com/bbdamodaran/deepJDOT>

2. <https://scikit-learn.org/stable/>

TABLE 2
Overall Evaluation Results

	MIMIC → Challenge		Challenge → MIMIC		Average
	AUC	improvement	AUC	improvement	improvement
<i>Source Only</i>					
LR	0.560	16.12%	0.728	4.28%	10.20%
NN	0.592	9.76%	0.705	7.70%	8.73%
XGBoost	0.608	6.82%	0.594	27.88%	17.35%
<i>Target Only</i>					
LR	0.602	7.89%	0.716	6.09%	6.99%
NN	0.559	16.26%	0.605	25.60%	20.93%
XGBoost	0.578	12.44%	0.730	4.03%	8.23%
<i>Source & Target Train Together</i>					
LR	0.599	8.50%	0.730	4.05%	6.28%
NN	0.609	6.70%	0.715	6.24%	6.47%
XGBoost	0.600	8.23%	0.687	10.65%	9.44%
<i>Source & Target Transfer</i>					
DeepJDOT	0.612	6.12%	0.726	4.69%	5.47%
Finetune	0.601	8.11%	0.716	6.05%	7.08%
SPSSOT	0.650	-	0.760	-	-

and the number of iterations is 5000. In *SPSSOT*, we set $\alpha = 0.05$ in Eq. (4), $\theta_s = 1.0$ in Eq.(5) and $\beta = 0.15$, $\lambda = 0.5$ in Eq. (9). The parameter sensitivity analysis is conducted later in Sec.5.5.3. In Algorithm 2, the hardness function is Squared Error, the number of base classifiers is set to 5, the number of bins is to 10 and the number of iterations is set to 1000. The results are reported by the mean results of 5 runs.

For assessment, we use the classification evaluation metric, Area Under Curve (AUC), which is a summary measure of sensitivity and specificity, that has been customary to the field of diagnostic test accuracy. Over 80% papers about Sepsis’s prediction reported AUC [27]. Therefore, we also pick it as our performance metric.

Our experiment platform is a server with AMD Ryzen 9 3900X 12-Core Processor, 64 GB RAM and GeForce RTX 3090. We use Python 3.8 with scikit-learn 0.24, POT 0.7 and tensorflow 2.4 on Ubuntu 20.04 for algorithm implementation. Code for our model can be found on Github ⁵.

5.4 Results and Discussion

The experiment results of *SPSSOT* and the baselines are reported in Table 2. For a more comprehensive comparison, we show the experimental results from three different perspectives.

First, *SPSSOT* outperforms the other two transfer learning baselines. Between them, *DeepJDOT* is an unsupervised transfer learning method based on Optimal Transport [24], and thus the improvement is expected because we provide a little labeled data in target domain in *SPSSOT*. Compared to *Finetune*, a common method in transfer learning, the advantage of our method further verifies the effectiveness of using optimal transport to align two feature spaces during the training process. It is worth noting that, while *Finetune* considers 1% labeled data in the target domain, its performance is even worse than *DeepJDOT* without considering any labeled target data. This indicates that even if we have certain labeled data in the target domain, it is still non-trivial to properly leverage the knowledge of such labeled data. Our research, by proposing a novel semi-supervised

OT transfer learning method *SPSSOT*, can leverage the little labeled target data more efficiently during the knowledge transfer process.

Second, compared to methods (*LR*, *NN* and *XGBoost*) that are trained with source data and target labeled data together, *SPSSOT* improves at least 6.70% in MIMIC → Challenge and 4.05% in Challenge → MIMIC. The probable reason is that the feature distributions of two domains have some differences so that putting them together to train a model directly is not effective. When we further compare models that *train together* and *Finetune*, it is obvious to find that *Finetune* may not perform better. This result illustrates that though the model trained with source data provides initial parameters for *FineTune*, the initialization probably is not suitable for target data. Therefore, it is common to appear a negative transfer when the feature distributions of two domains are not similar.

Third, all the no-transfer baselines, i.e., *Source Only* and *Target Only*, perform rather poorly. The results of *Source Only* indicate that, though MIMIC and Challenge both are medical datasets with the same features, there still are some differences. And if we only have a small amount of labeled data (1% in our setting) to train the model, the performance can not be guaranteed, which is like the *cold start* scenario. Also, we can find the AUC values of *NN* are very small while only using target labeled data, which may be due to *NN* overfitting on a small number of samples.

5.5 Analysis

5.5.1 Ablation Study

To analyse the separate contribution of *SPSSOT*, we compare *SPSSOT* with three variants of *SPSSOT* in this section, as listed below:

- *SSOT*: we remove Self-paced ensemble from the full model.
- *SPSSOT_NC*: we do not consider intra-domain structure during transferring, i.e., $\beta = 0$ in Eq. (9).
- *SPSSOT_NG*: we delete the group entropic loss during training, i.e., $\lambda = 0$ in Eq. (9).

5. <https://github.com/RuiqingDing/SPSSOT>

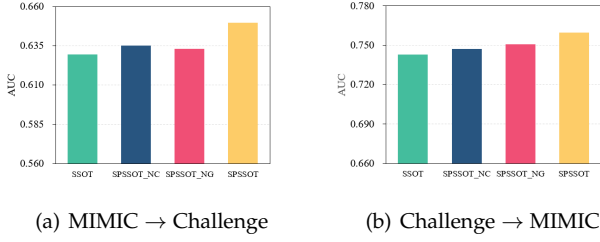


Fig. 4. Ablation Study.

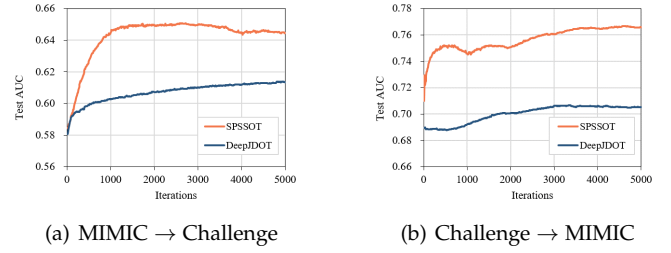
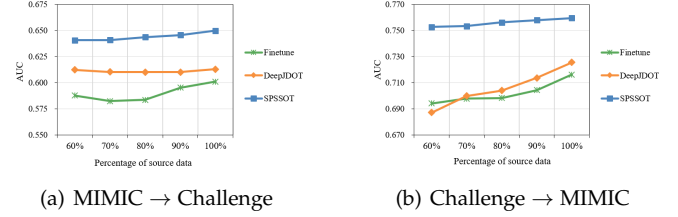
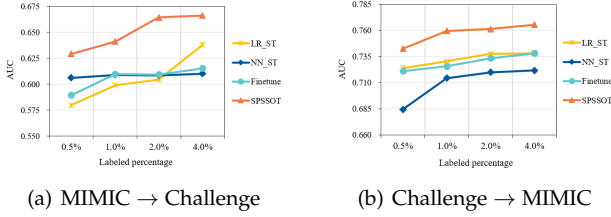
Fig. 5. The convergence performance of *SPSSOT* and *DeepJDOT*.

Fig. 6. Results with different percentages of labeled data in target domain. Fig. 7. Results with different sampling percentages of source data.

The results are shown in Fig. 4. As we can see, compared with the complete model, *SSOT* is worse because after removing the Self-paced ensemble, the datasets encounter an imbalance that will result in the difficulty of modeling. And *SSPSOT_NC* ignores the intra-domain structure with no consideration of the embedding distances in the hidden feature space, making it is hard to find a good classification boundary. What's more, *SPSSOT_NG* causes the paired samples may come from different classes for unlabeled samples in the target domain, which would lead to an ambiguous result. In brief, the results indicate that each part of our model *SPSSOT* is necessary.

5.5.2 Convergence

To illustrate the convergence of *SPSSOT*, we evaluate the test AUCs of the transfer methods, *SPSSOT* and *DeepJDOT*. The results are shown in Fig. 5. It reveals that our model can achieve significantly better test AUCs only with a few iterations and keep relatively stable convergence performance. Also, on the task of Challenge → MIMIC, we can find there are obvious changes in some iterations, like the 1000th and the 2000th iterations. That is because after 1000 iterations of *SPSSOT*, we will resample from the majority data and continue to train iteratively. Also, with the increasing re-sampling times, the performance of test data will gradually become stable.

5.5.3 Sensitivity Analysis

Labeled Percentage in Target Domain. In experiments, we set 1% of the target domain data to have labels by default. To further verify the stability of the method, we adjust the proportion of samples with known labels in the target domain to 0.5%, 2% and 4%. In Fig. 6, we show the results of different models in different labeled percentages. It can be observed that whether or not the source domain is Challenge or MIMIC, *SPSSOT* always performs best in these percentages (the top line). It is reasonable that as the labeled

percentage decreases, so does the models' performances. However, compared with models that train with source data and target labeled data, *SPSSOT* keeps a relatively steady trend. This is an ideal situation for practical application, which means that we can train a transfer model with acceptable performance by spending a small amount of cost to label a small amount of data.

Sampling Percentage of Source Data. To validate the effect of different numbers of source domain samples, we conduct experiments on source data with different sample sizes. Fig. 7 displays the results, whose abscissa indicates the sampling percentage from original source data. We observe that the performance of all methods increases when using more source samples. At the same time, Our *SPSSOT* approach consistently outperforms the other two baselines, which demonstrates the effectiveness of our proposed method for transfer.

Hyper-parameter Sensitivity. There exists four important hyper-parameters in the loss function of *SPSSOT*: the weight of optimal transport α in Eq. (4), the weight of the source data's classification loss θ_s in Eq. (5), the weight of discriminative centroid loss β and the weight of group entropy λ in Eq. (9). To test the stability of the performances of *SPSSOT*, we test different values of α , θ_s , β and λ on both two transfer scenarios, i.e., Challenge → MIMIC and MIMIC → Challenge. The results are shown in Fig. 8. Comparatively speaking, it is not very sensitive to β in both scenarios. As the other parameters change, the results have some fluctuations. According to the performance, we select the values of these parameters used in the model actually, i.e., $\alpha = 0.05$, $\theta_s = 1$, $\beta = 0.15$ and $\lambda = 0.5$.

5.5.4 Feature visualization

To show the feature transfer capability, we also visualize the t-SNE embeddings [58] of the hidden representation by *Finetune*, *DeepJDOT* and *SPSSOT* on both transfer scenarios. Fig. 9 (a) - 9 (c) correspond to MIMIC → Challenge and

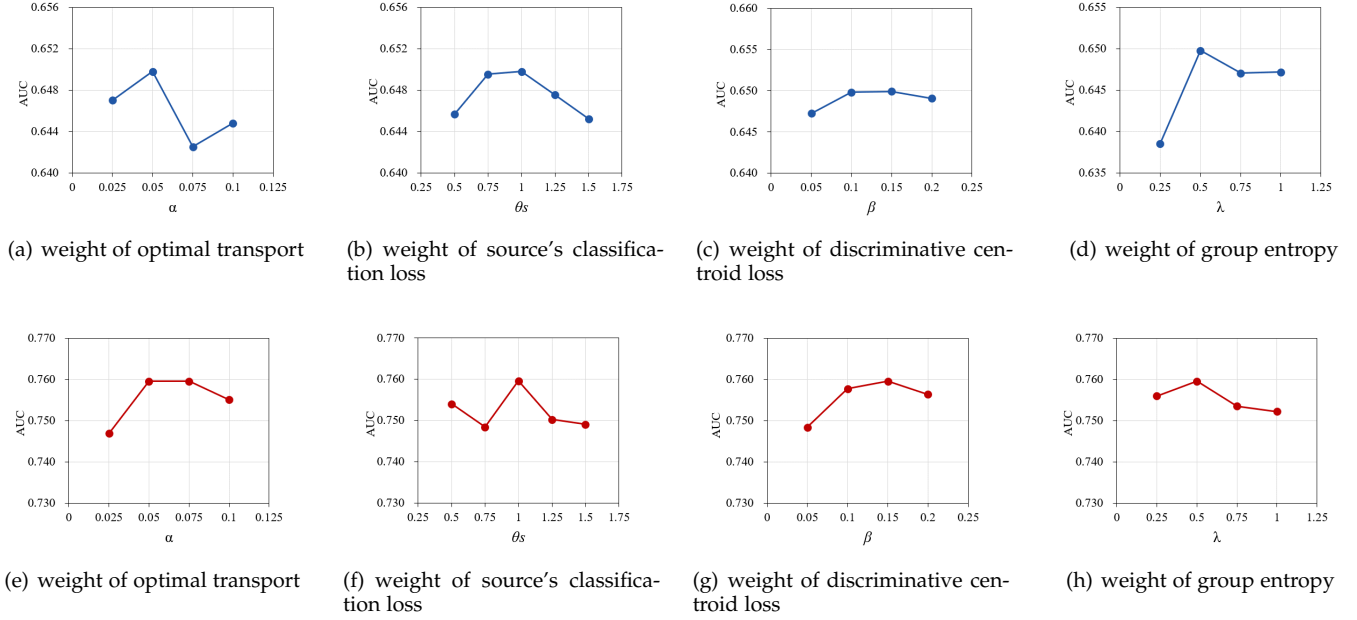


Fig. 8. Parameter Sensitivity. Figures (a) - (d) in the first row correspond to MIMIC \rightarrow Challenge, and Figures (e) - (h) in the second row correspond to Challenge \rightarrow MIMIC.

Fig. 9 (d) - 9 (f) correspond to Challenge \rightarrow MIMIC. In each sub-figure, different colors denote different categories (red: will have Sepsis, blue: will not have Sepsis), and different shapes denote different domains (round: source domain, cross: target). Fig. 9(a) and Fig. 9(d) display that the features learned by *Finetune* for different domains are almost totally separated, i.e., points represented by different shapes in the same feature space are separated from each other. Fig. 9(b) and Fig. 9(e) illustrate that though the domains can be aligned to a certain extent, the bad thing is some target samples are aligned to the source data with wrong classes, causing negative transfer. Note that, Fig. 9(c) and Fig. 9(f) show that the features generated by *SPSSOT* achieve better domain alignment with a clearer class boundary. The visualization results reveal that our proposal can match the complex structures of the source and target domains as well as maximize the margin between different classes.

6 CONCLUSION

In this paper, we describe a new framework based on optimal transport and self-paced ensemble to solve the semi-supervised transfer learning problem for Sepsis early detection in the scenario that there is only little labeled data in the target domain (e.g. hospital). Empirical studies on real-world clinical datasets demonstrate the effectiveness of the proposed *SPSSOT* algorithm in aligning two feature spaces and eliminating the influence of class imbalance. In fact, though *SPSSOT* is proposed for Sepsis early detection, our work can be easily adapted for many other transfer learning tasks. The only requirement for *SPSSOT* to work is choosing a suitable structure to extract deep features, e.g., CNNs for image identification [43] and RNNs for time series prediction [59].

It is no doubt that there are still many problems to be solved. First, we can further explore how to extend *SPSSOT*

to the transfer situation with multi-source domains. Now we only consider transferring knowledge from one source domain. Besides, we can try other popular deep neural network structures as the feature generator. For the prediction of Sepsis, we can regard the physiological indicators in a period of time before the occurrence of Sepsis as time-series data, then we can use some structures designed for time series, including LSTM [59], GRU [60] and so on. Finally, privacy protection is an important problem that can not be ignored when models are implemented in real-world applications because a large amount of training data is often required to ensure the performance and robustness of the models. However, the constraints of privacy protection clauses often prevent data from being moved to the data center for unified storage and training, so federated learning [61] provides a new idea and still needs to be explored.

APPENDIX A FEATURE DESCRIPTION

In this section, we list the features we used in our model and give a brief description of each features. The details are shown in Table 3.

ACKNOWLEDGMENTS

This work is supported by grants from the National Natural Science Foundation of China (No. 81801940 Y.Z.).

REFERENCES

- [1] M. Singer, C. S. Deutschman, C. W. Seymour, M. Shankar-Hari, D. Annane, M. Bauer, R. Bellomo, G. R. Bernard, J.-D. Chiche, C. M. Coopersmith, R. S. Hotchkiss, M. M. Levy, J. C. Marshall, G. S. Martin, S. M. Opal, G. D. Rubenfeld, T. van der Poll, J.-L. Vincent, and D. C. Angus, "The Third International Consensus Definitions for Sepsis and Septic Shock (Sepsis-3)," *JAMA*, vol. 315, no. 8, pp. 801-810, 02 2016. [Online]. Available: <https://doi.org/10.1001/jama.2016.0287>

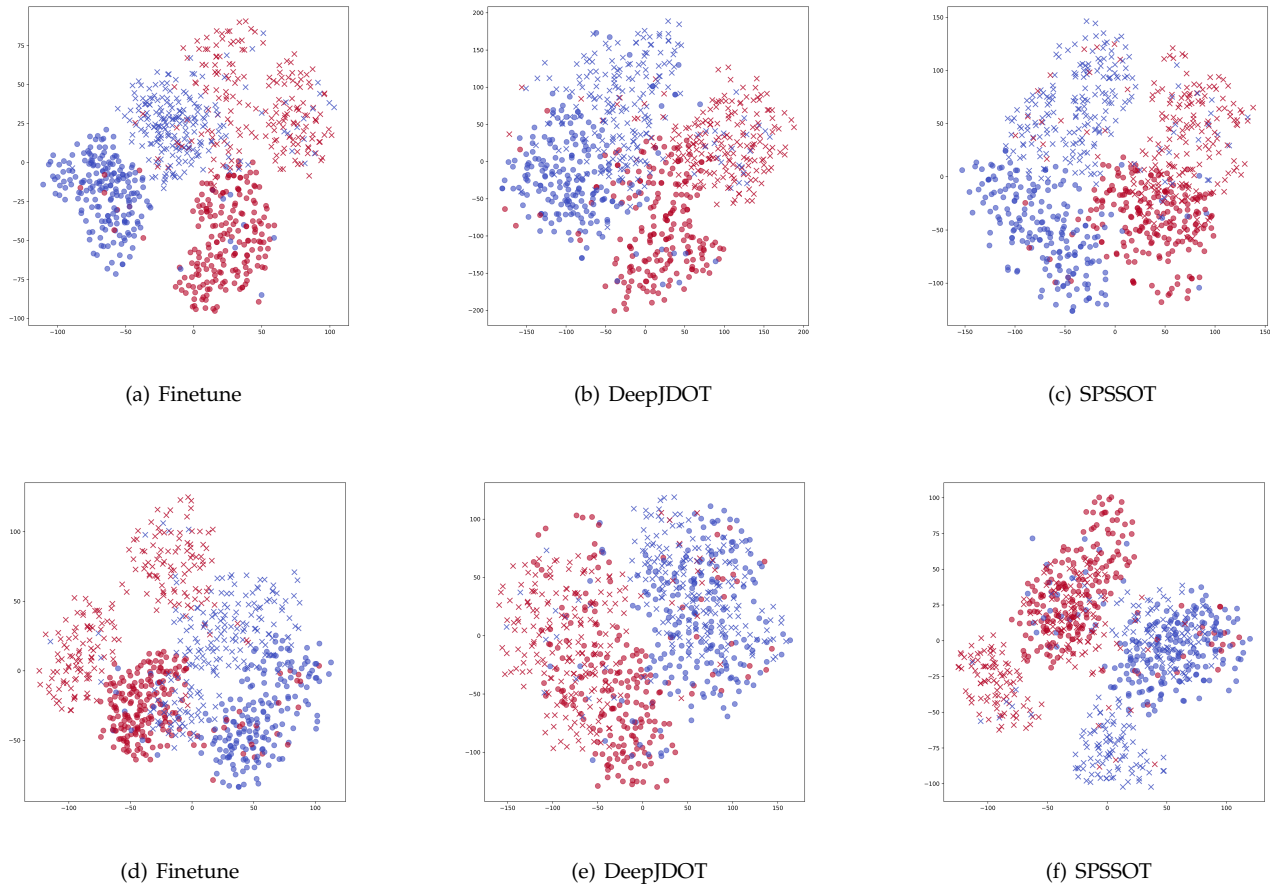


Fig. 9. Feature visualization. Figures (a) - (c) in the first row corresponds to MIMIC \rightarrow Challenge, and Figures (d) - (f) in the second row corresponds to Challenge \rightarrow MIMIC. Different colors represent different classes (red: will have Sepsis, blue: will not have Sepsis), different shapes represent different domains (round: source domain, cross: target). *Best viewed in color.*

- [2] J. J. Zimmerman, "Pediatric sepsis from start to finish," *Pediatric critical care medicine: a journal of the Society of Critical Care Medicine and the World Federation of Pediatric Intensive and Critical Care Societies*, vol. 16, no. 5, p. 479, 2015.
- [3] C. Fleischmann, A. Scherag, N. K. Adhikari, C. S. Hartog, T. Tsaganos, P. Schlattmann, D. C. Angus, and K. Reinhart, "Assessment of global incidence and mortality of hospital-treated sepsis. current estimates and limitations," *American journal of respiratory and critical care medicine*, vol. 193, no. 3, pp. 259–272, 2016.
- [4] L. Ou, J. Chen, K. Hillman, A. Flabouris, M. Parr, H. Assareh, and R. Bellomo, "The impact of post-operative sepsis on mortality after hospital discharge among elective surgical patients: a population-based cohort study," *Critical Care*, vol. 21, no. 1, pp. 1–13, 2017.
- [5] E. Sheerit, N. Nissim, D. Klimov, L. Fuchs, Y. Elovici, and Y. Shahr, "Temporal pattern discovery for accurate sepsis diagnosis in icu patients," *arXiv preprint arXiv:1709.01720*, 2017.
- [6] A. Kumar, D. Roberts, K. E. Wood, B. Light, J. E. Parrillo, S. Sharma, R. Suppes, D. Feinstein, S. Zanotti, L. Taiberg *et al.*, "Duration of hypotension before initiation of effective antimicrobial therapy is the critical determinant of survival in human septic shock," *Critical care medicine*, vol. 34, no. 6, pp. 1589–1596, 2006.
- [7] S. P. Shashikumar, M. D. Stanley, I. Sadiq, Q. Li, A. Holder, G. D. Clifford, and S. Nemat, "Early sepsis detection in critical care patients using multiscale blood pressure and heart rate dynamics," *Journal of electrocardiology*, vol. 50, no. 6, pp. 739–743, 2017.
- [8] S. Hornig, D. A. Sontag, Y. Halpern, Y. Jernite, N. I. Shapiro, and L. A. Nathanson, "Creating an automated trigger for sepsis clinical decision support at emergency department triage using machine learning," *PloS one*, vol. 12, no. 4, p. e0174708, 2017.
- [9] J. Futoma, S. Hariharan, and K. Heller, "Learning to detect sepsis with a multitask gaussian process rnn classifier," in *International Conference on Machine Learning*. PMLR, 2017, pp. 1174–1182.
- [10] X. Li, X. Xu, F. Xie, X. Xu, Y. Sun, X. Liu, X. Jia, Y. Kang, L. Xie, F. Wang *et al.*, "A time-phased machine learning model for real-time prediction of sepsis in critical care," *Critical Care Medicine*, vol. 48, no. 10, pp. e884–e888, 2020.
- [11] S. J. Pan and Q. Yang, "A survey on transfer learning," *IEEE Transactions on knowledge and data engineering*, vol. 22, no. 10, pp. 1345–1359, 2009.
- [12] G. Lee, I. Rubinfeld, and Z. Syed, "Adapting surgical models to individual hospitals using transfer learning," in *2012 IEEE 12th international conference on data mining workshops*. IEEE, 2012, pp. 57–63.
- [13] E. Choi, M. T. Bahadori, A. Schuetz, W. F. Stewart, and J. Sun, "Doctor ai: Predicting clinical events via recurrent neural networks," in *Machine learning for healthcare conference*. PMLR, 2016, pp. 301–318.
- [14] J. Y. Lee, F. Dernoncourt, and P. Szolovits, "Transfer learning for named-entity recognition with neural networks," *arXiv preprint arXiv:1705.06273*, 2017.
- [15] P. Gupta, P. Malhotra, J. Narwariya, L. Vig, and G. Shroff, "Transfer learning for clinical time series analysis using deep neural networks," *Journal of Healthcare Informatics Research*, vol. 4, no. 2, pp. 112–137, 2020.
- [16] H. S. Luft, D. W. Garnick, D. H. Mark, D. J. Peltzman, C. S. Phibbs, E. Lichtenberg, and S. J. McPhee, "Does quality influence choice of hospital?" *Jama*, vol. 263, no. 21, pp. 2899–2906, 1990.
- [17] S. J. Pan, I. W. Tsang, J. T. Kwok, and Q. Yang, "Domain adaptation via transfer component analysis," *IEEE Transactions on Neural Networks*, vol. 22, no. 2, pp. 199–210, 2010.
- [18] K. Azzadenesheli, A. Liu, F. Yang, and A. Anandkumar, "Regu-

TABLE 3
All features used in model

	Measurement	Description
Vital sign variables	HR	Heart rate (beats per minute) s
	O2Sat	Pulse oximetry (%)
	Temp	Temperature (deg C)
	SBP	Systolic BP (mm Hg)
	MAP	Mean arterial pressure (mm Hg)
	DBP	Diastolic BP (mm Hg)
	Resp	Respiration rate (breaths per minute)
Laboratory variables	BaseExcess	Excess bicarbonate (mmol/L)
	HCO3	Bicarbonate (mmol/L)
	FiO2	Fraction of inspired oxygen (%)
	pH	pH
	PaCO2	The partial pressure of carbon dioxide from arterial blood (mm Hg)
	SaO2	Oxygen saturation from arterial blood (%)
	AST	Aspartate transaminase (IU/L)
	BUN	Blood urea nitrogen (mg/dL)
	Alkalinephos	Alkaline phosphatase (IU/L)
	Calcium	Calcium (mg/dL)
	Chloride	Chloride (mmol/L)
	Creatinine	Creatinine (mg/dL)
	Bilirubin direct	Direct bilirubin (mg/dL)
	Glucose	Serum glucose (mg/dL)
	Lactate	Lactic acid (mg/dL)
	Magnesium	Magnesium (mmol/dL)
	Phosphate	Phosphate (mg/dL)
	Potassium	Potassium (mmol/L)
	Bilirubin total	Total bilirubin (mg/dL)
	TroponinI	Troponin I (ng/mL)
	Hct	Hematocrit (%)
	Hgb	Hemoglobin (g/dL)
	PTT	Partial thromboplastin time (seconds)
	WBC	Leukocyte count (count/L)
	Platelets	Platelet count (count/mL)
Demographic variables	Age	Age (years)
	Sex	Female (0) or male (1)
	HospAdmTime	The time between hospital and ICU admission (hours since ICU admission)
	ICULOS	ICU length of stay (hours since ICU admission)

larized learning for domain adaptation under label shifts." in *ICLR (Poster)*, 2019.

- [19] C. Cortes, Y. Mansour, and M. Mohri, "Learning bounds for importance weighting," in *Nips*, vol. 10. Citeseer, 2010, pp. 442–450.
- [20] C. Cortes and M. Mohri, "Domain adaptation and sample bias correction theory and algorithm for regression," *Theoretical Computer Science*, vol. 519, pp. 103–126, 2014.
- [21] M. Buda, A. Maki, and M. A. Mazurowski, "A systematic study of the class imbalance problem in convolutional neural networks," *Neural Networks*, vol. 106, pp. 249–259, 2018.
- [22] Y. Yang and Z. Xu, "Rethinking the value of labels for improving class-imbalanced learning," in *Conference on Neural Information Processing Systems (NeurIPS)*, 2020.
- [23] Z. Liu, W. Cao, Z. Gao, J. Bian, H. Chen, Y. Chang, and T.-Y. Liu, "Self-paced ensemble for highly imbalanced massive data classification," in *2020 IEEE 36th International Conference on Data Engineering (ICDE)*. IEEE, 2020, pp. 841–852.
- [24] B. B. Damodaran, B. Kellenberger, R. Flamary, D. Tuia, and N. Courty, "Deepjdot: Deep joint distribution optimal transport for unsupervised domain adaptation," in *Proceedings of the European Conference on Computer Vision (ECCV)*, 2018, pp. 447–463.
- [25] G. Monge, "Mémoire sur la théorie des déblais et des remblais," *Histoire de l'Académie Royale des Sciences de Paris*, 1781.
- [26] C. Villani, *Optimal transport: old and new*. Springer Science & Business Media, 2008, vol. 338.
- [27] L. M. Fleuren, T. L. Klausch, C. L. Zwager, L. J. Schoonmade, T. Guo, L. F. Roggeveen, E. L. Swart, A. R. Girbes, P. Thorat, A. Ercole *et al.*, "Machine learning for the prediction of sepsis: a systematic review and meta-analysis of diagnostic test accuracy," *Intensive care medicine*, vol. 46, no. 3, pp. 383–400, 2020.
- [28] A. Karpatne, I. Ebert-Uphoff, S. Ravela, H. A. Babaie, and V. Kumar, "Machine learning for the geosciences: Challenges and opportunities," *IEEE Transactions on Knowledge and Data Engineering*, vol. 31, no. 8, pp. 1544–1554, 2018.
- [29] M. A. Reyna, C. Josef, S. Seyed, R. Jeter, S. P. Shashikumar, M. B. Westover, A. Sharma, S. Nemati, and G. D. Clifford, "Early prediction of sepsis from clinical data: the physionet/computing in cardiology challenge 2019," in *2019 Computing in Cardiology (CinC)*. IEEE, 2019, pp. Page–1.
- [30] M. Yang, C. Liu, X. Wang, Y. Li, H. Gao, X. Liu, and J. Li, "An explainable artificial intelligence predictor for early detection of sepsis," *Critical Care Medicine*, vol. 48, no. 11, pp. e1091–e1096, 2020.
- [31] M. Komorowski, L. A. Celi, O. Badawi, A. C. Gordon, and A. A. Faisal, "The artificial intelligence clinician learns optimal treatment strategies for sepsis in intensive care," *Nature medicine*, vol. 24, no. 11, pp. 1716–1720, 2018.
- [32] N. Tomašev, X. Glorot, J. W. Rae, M. Zielinski, H. Askham, A. Saraiva, A. Mottram, C. Meyer, S. Ravuri, I. Protsyuk *et al.*, "A clinically applicable approach to continuous prediction of future acute kidney injury," *Nature*, vol. 572, no. 7767, pp. 116–119, 2019.
- [33] S. L. Hyland, M. Faltys, M. Hüser, X. Lyu, T. Gumbsch, C. Esteban, C. Bock, M. Horn, M. Moor, B. Rieck *et al.*, "Early prediction of circulatory failure in the intensive care unit using machine learning," *Nature medicine*, vol. 26, no. 3, pp. 364–373, 2020.
- [34] P. S. Roshanov, G. H. Guyatt, V. Tandon, F. K. Borges, A. Lamy, R. Whitlock, B. M. Biccand, W. Szczeklik, M. Panju, J. Spence *et al.*, "Preoperative prediction of bleeding independently associated with mortality after noncardiac surgery (bims): an international

- prospective cohort study," *British Journal of Anaesthesia*, vol. 126, no. 1, pp. 172–180, 2021.
- [35] M. C. Moghadam, E. M. K. Abad, N. Bagherzadeh, D. Ramsingh, G.-P. Li, and Z. N. Kain, "A machine-learning approach to predicting hypotensive events in icu settings," *Computers in biology and medicine*, vol. 118, p. 103626, 2020.
- [36] N. Courty, R. Flamary, D. Tuia, and A. Rakotomamonjy, "Optimal transport for domain adaptation," *IEEE transactions on pattern analysis and machine intelligence*, vol. 39, no. 9, pp. 1853–1865, 2016.
- [37] N. Courty, R. Flamary, and D. Tuia, "Domain adaptation with regularized optimal transport," in *Joint European Conference on Machine Learning and Knowledge Discovery in Databases*. Springer, 2014, pp. 274–289.
- [38] M. Perrot, N. Courty, R. Flamary, and A. Habrard, "Mapping estimation for discrete optimal transport," in *Proceedings of the 30th International Conference on Neural Information Processing Systems*, 2016, pp. 4204–4212.
- [39] I. Redko, A. Habrard, and M. Sebban, "Theoretical analysis of domain adaptation with optimal transport," in *Joint European Conference on Machine Learning and Knowledge Discovery in Databases*. Springer, 2017, pp. 737–753.
- [40] N. Courty, R. Flamary, A. Habrard, and A. Rakotomamonjy, "Joint distribution optimal transportation for domain adaptation," in *NIPS 2017*, 2017.
- [41] Y. Yan, W. Li, H. Wu, H. Min, M. Tan, and Q. Wu, "Semi-supervised optimal transport for heterogeneous domain adaptation," in *IJCAI*, vol. 7, 2018, pp. 2969–2975.
- [42] R. Flamary, N. Courty, A. Gramfort, M. Z. Alaya, A. Boisbunon, S. Chambon, L. Chapel, A. Corenflos, K. Fatras, N. Fournier, L. Gautheron, N. T. Gayraud, H. Janati, A. Rakotomamonjy, I. Redko, A. Rolet, A. Schutz, V. Seguy, D. J. Sutherland, R. Tavenard, A. Tong, and T. Vayer, "Pot: Python optimal transport," *Journal of Machine Learning Research*, vol. 22, no. 78, pp. 1–8, 2021. [Online]. Available: <http://jmlr.org/papers/v22/20-451.html>
- [43] R. Xu, P. Liu, L. Wang, C. Chen, and J. Wang, "Reliable weighted optimal transport for unsupervised domain adaptation," in *Proceedings of the IEEE/CVF Conference on Computer Vision and Pattern Recognition*, 2020, pp. 4394–4403.
- [44] C. Cortes and V. Vapnik, "Support-vector networks," *Machine learning*, vol. 20, no. 3, pp. 273–297, 1995.
- [45] C.-T. Lin, C. S. G. Lee *et al.*, "Neural-network-based fuzzy logic control and decision system," *IEEE Transactions on computers*, vol. 40, no. 12, pp. 1320–1336, 1991.
- [46] C. Elkan, "The foundations of cost-sensitive learning," in *International joint conference on artificial intelligence*, vol. 17, no. 1. Lawrence Erlbaum Associates Ltd, 2001, pp. 973–978.
- [47] T.-Y. Lin, P. Goyal, R. Girshick, K. He, and P. Dollár, "Focal loss for dense object detection," in *Proceedings of the IEEE international conference on computer vision*, 2017, pp. 2980–2988.
- [48] N. V. Chawla, A. Lazarevic, L. O. Hall, and K. W. Bowyer, "Smoteboost: Improving prediction of the minority class in boosting," in *European conference on principles of data mining and knowledge discovery*. Springer, 2003, pp. 107–119.
- [49] N. V. Chawla, K. W. Bowyer, L. O. Hall, and W. P. Kegelmeyer, "Smote: synthetic minority over-sampling technique," *Journal of artificial intelligence research*, vol. 16, pp. 321–357, 2002.
- [50] Y. Freund, R. E. Schapire *et al.*, "Experiments with a new boosting algorithm," in *icml*, vol. 96. Citeseer, 1996, pp. 148–156.
- [51] A. L. Goldberger, L. A. Amaral, L. Glass, J. M. Hausdorff, P. C. Ivanov, R. G. Mark, J. E. Mietus, G. B. Moody, C.-K. Peng, and H. E. Stanley, "Physiobank, physiotoolkit, and physionet: components of a new research resource for complex physiologic signals," *circulation*, vol. 101, no. 23, pp. e215–e220, 2000.
- [52] C. W. Seymour, V. X. Liu, T. J. Iwashyna, F. M. Brunkhorst, T. D. Rea, A. Scherag, G. Rubenfeld, J. M. Kahn, M. Shankar-Hari, M. Singer, C. S. Deutschman, G. J. Escobar, and D. C. Angus, "Assessment of Clinical Criteria for Sepsis: For the Third International Consensus Definitions for Sepsis and Septic Shock (Sepsis-3)," *JAMA*, vol. 315, no. 8, pp. 762–774, 02 2016. [Online]. Available: <https://doi.org/10.1001/jama.2016.0288>
- [53] S. Angenent, S. Haker, and A. Tannenbaum, "Minimizing flows for the monge-kantorovich problem," *SIAM journal on mathematical analysis*, vol. 35, no. 1, pp. 61–97, 2003.
- [54] Y. Wen, K. Zhang, Z. Li, and Y. Qiao, "A discriminative feature learning approach for deep face recognition," in *European conference on computer vision*. Springer, 2016, pp. 499–515.
- [55] D. Gamberger, N. Lavrac, and C. Groselj, "Experiments with noise filtering in a medical domain," in *ICML*, vol. 99, 1999, pp. 143–151.
- [56] A. E. Johnson, T. J. Pollard, L. Shen, H. L. Li-Wei, M. Feng, M. Ghassemi, B. Moody, P. Szolovits, L. A. Celi, and R. G. Mark, "Mimic-iii, a freely accessible critical care database," *Scientific data*, vol. 3, no. 1, pp. 1–9, 2016.
- [57] M. Zabihi, S. Kiranyaz, and M. Gabbouj, "Sepsis prediction in intensive care unit using ensemble of xgboost models," in *2019 Computing in Cardiology (CinC)*. IEEE, 2019, pp. Page–1.
- [58] L. Van der Maaten and G. Hinton, "Visualizing data using t-sne," *Journal of machine learning research*, vol. 9, no. 11, 2008.
- [59] S. Hochreiter and J. Schmidhuber, "Long short-term memory," *Neural computation*, vol. 9, no. 8, pp. 1735–1780, 1997.
- [60] J. Chung, C. Gulcehre, K. Cho, and Y. Bengio, "Empirical evaluation of gated recurrent neural networks on sequence modeling," *arXiv preprint arXiv:1412.3555*, 2014.
- [61] Q. Yang, Y. Liu, T. Chen, and Y. Tong, "Federated machine learning: Concept and applications," *ACM Transactions on Intelligent Systems and Technology (TIST)*, vol. 10, no. 2, pp. 1–19, 2019.